

BRAZILIAN CLAYS AS POTENTIAL BUFFER MATERIALS FOR RADIOACTIVE WASTE FINAL STORAGE

Gabo G. Machado*¹, Sabine N. Guilhen², Victoria V. Krupskaya³, Sergey V. Zakusin³, Ekaterina A. Tyupina⁴, Julio Harada⁵, Roberto Vicente², Rodrigo P. de Souza⁶, Leandro G. Araujo², Denise C. R. Espinosa¹

¹ Depto. de Engenharia Química da Escola Politécnica da Universidade de São Paulo (POLI/USP)
Rua do Lago, 250 – 05508-080 São Paulo, Brazil
gabo.machado@usp.br, espinosa@usp.br

²Instituto de Pesquisas Energéticas e Nucleares (IPEN/CNEN-SP)
Av. Prof. Lineu Prestes 2242 – 05508-000 São Paulo, SP, Brazil
snguilhen@ipen.br, rvicente@ipen.br, lgoulart@usp.br

³Institute of Geology of Ore Deposits, Petrography, Mineralogy and Geochemistry, Russian Academy of Sciences (IGEM RAS)
Staromonetny Pereulok, 35 – 119017 Moscow, Russia
krupskaya@ruclay.com

⁴Mendeleev University of Chemical Technology of Russia (RCTU)
Miusskaya Ploshchad', 9 – 125047 Moscow, Russia
tk1972@mail.ru, zakusinsergey@gmail.com

⁵Depto. de Nanociências e Materiais Avançados, Universidade Federal do ABC
Av. dos Estados, 5001 – 09210-580 Santo André, SP, Brazil
harada.julio@terra.com.br

⁶Instituto de Pesquisas Tecnológicas do Estado de São Paulo (IPT)
Av. Prof. Almeida Prado, 532 – 05508-901 São Paulo, SP, Brazil
rodrigopapai@ipt.br

ABSTRACT

Clayey materials have been adopted in most nuclear waste producing countries, as a key constituent in engineered barrier for final disposal facilities at all levels of radioactive wastes (LILW-SL, LILW-LL and HLW). The following study presents a thorough characterization upon five Brazilian clay rich deposits, mostly smectite bearing clays, aiming to evaluate their expected performance as clay buffer under the conditions associated to a Low and Intermediate Level Waste Repository (RBMN); being the former a matter of national strategic interest. Samples coming from the Brazilian states of Bahia, Maranhão, Pará and Paraíba were treated and analyzed by means of X-Ray diffraction as a main technique, and complemented by FTIR, LALLS, XRF and SEM-EDS, in order to establish mineralogical composition, particle size distribution and chemical composition. Moreover, several standard clay treatments over the <1 μm size fraction were carried out to reveal information regarding layer charge, major interlayer cations, unit formula and other crystal features of smectite species present in a mineralogical assembly, enabling the construction of a molecular model over which would be realistic to simulate the diffusion of radionuclides. Results obtained on ^{133}Cs adsorption experiments indicate that mineralogical composition would probably be the single most influential factor controlling transport capacity of positively charged radionuclides in the current setup, and can be expressed in terms of smectite contents, favoring montmorillonite rich materials containing majorly Na^+ as compensating cation in interlayer position. Thus, the obtained data will be useful in the testing of optimal compaction conditions to obtain the most suitable buffer material for the repository design. However, this trend is yet to be contrasted against hydraulic conductivity measurements and swelling pressure to see how they match.

1. INTRODUCTION

A variety of activities generate radioactive wastes that needs to be properly managed for environment and human safeguard. Normally, these wastes need to be isolated for many years in a proper containment structure until they decay to safe levels for final disposal known as geologic disposal [1]. In this type of shelters, it is often found the use of smectite rich clays in order to embed waste fuel canisters as “clay buffer”, due to the following special properties: Low hydraulic conductivity, low anion diffusion capacity, low transport capacity, high swelling (and therefore enhance sealing capability if installed in a dry and highly compacted state), colloidal filtering properties, microbes filtering properties [2] and many other marvelous features of this naturally occurring nanoparticles.

In LILW disposal facilities, the standard containing infrastructures does not has to respond for such a long lifetime and consequently, other enhance applications of clay minerals apply such and clay liners, top cover bentonite/sand mix, filled or granulated smectite powder, etc.

The Brazilian nuclear waste legacy generated by Angra 1 and 2 power reactors are currently in interim storage on site at Central Nuclear Almirante Álvaro Alberto in Itaorna (Angra dos Reis, RJ, Brazil). This storage’s capacity is expected to be exceeded between 2020 and 2025, raising concerns for a definitive repository construction. A preferred option for this question is the disposal in surface or near surface facilities that would allow for long term storage of LILW. In these facilities, the radioactive waste would be placed in mineral or natural cavities some tens of meters below the surface [3]. The National Commission of Nuclear Energy (CNEN) is responsible for the regulation of radioactive waste storage and management. In 2009, they started a project called “Low and Intermediate Level Waste Repository” (RBMN) aiming the construction of a repository for the Angra powerplants radioactive wastes [4, 5].

Cesium-137 is one of the radioactive fission products of most concern due to its high solubility, cesium can contaminate large volumes of water, being efficiently taken up by plants and absorbed by animals for its similarity to potassium, an essential nutrient [6, 7, 8, 9]. Therefore, an efficient containment is very important to prevent cesium transport to the environment and consequently living organisms such as humans themselves. Cesium presents the tendency to bond to clay minerals in soils and sediments [10]. It is strongly adsorbed onto illites or hydroxyinterlayered vermiculite [11, 12].

2. MATERIALS AND METHODS

2.1 Clay sources

For the current research project, a set of five samples representing most promising candidate clays for the purpose here being, and located within Brazil's national borders have been specifically selected, and listed in Table 1 as a function of their geological context. Most of them may be characterized as bentonites with the exception of sample coming from Parana, with can be described as a clay rich material with detrital amounts of smectite; and the rest may be considered low to mid-grade polycationic bentonites.

Table 1: List of samples arranged by geological areas.

Sample	Location	Comum name	Age	Parent rock	Formation Mode	Pos-Events
PA	Parana	Parana Raw	Mid-Permian	Ryolite/Dacite	InSitu Alteration	wethering/Illitization
BA	Bahia	Verde Duro	Tertiary	Basalt	In situ or Hydrothermal*	Uncertain
PA2	Paraiba	Verde macia	Tertiary	Basalt	In situ or Hydrothermal*	Uncertain
PA1	Paraiba	Chocolata	Tertiary	Basalt	Uncertain	Uncertain
MA	Maranhao	Maranhao	Triassic	Basalt	Hydrothermal or wethering*	Wethering

Samples have been designated as abbreviations of their respective origins, for instance, "BA" indicating the clay extracted in Bahia state, and so on.

2.2 Clay preparation

Clay preparation involved oven-drying of 1 kg/sample at 105 °C during 24 h, followed by grinding in a ceramic ball mill at 120 rpm and sieving till 100% passing 100 Mesh (100 % Wt < 149 µm). Afterwards, sub-sampling was carried out in a spinning riffler (Microscal Ltd.) to ensure representability. No Na activation was performed, neither acid attack to reduce soluble salt concentration and no H₂O₂ was used to remove oxidation and reduction potential of any remaining impurities.

Observations over the <1 µm size fraction was proceeded by size fractioning via sedimentation, after drying the material was pulverized up to 100% Wt < 74 µm (200 Mesh) using a Herzog pneumatic mill (HERZOG Automation Corp., Cleveland, OH, USA) for XRF, SEM and FTIR analysis. Smaller sample sizes (up to < 10 µm) were used in powder XRD for optimum setup [13, 14, 15].

2.3 Size distribution analysis

Size distribution of the clay samples will not only provide valuable information regarding mineral size populations, as also a frame or a sedimentation strategy. The analyses were performed for all bulk samples on a Malvern Mastersizer 2000 (Malvern Panalytical Ltd., Malvern). The tests were conducted without dispersant. The bulk samples were added in deionized water while applying an 1-minute intermittent ultrasonic treatment. The pumping speed was maintained at 2500 rpm.

2.4 Crystal structure analysis

X-ray diffraction (XRD) was carried out in a Bruker D8 Endeavour diffractometer (Bruker Corporation, Billerica, MA, USA) with a Cu anode using Co K α radiation (1.54 Å) at 40.0 kV and 40.0 mA over the range (2 θ) of 2–75° with a scan time of 0.5° min⁻¹, multilayer graphite monochromator and 2.3 mm soller slit for both incident and diffracted beam.

Bulk samples were prepared as “randomly oriented powder” (ROP) by backload on holders having 10 mm of sample surface, and less than 1 μ m size fraction as oriented slides (OS) on glass rounded slides of 25 mm. Most XRD protocols according to Moore and Reynolds [16] and Chipera and Bish [17].

Phase identification was performed using Bruker’s Software “Diffrac.Suite.Eva”(Version 4.1.1) and crystallographic information files PDF4 (2012) data base. Semi-quantitative phase analyzes were performed by the total multiphase spectrum refinement method (Rietveld method) using Bruker’s Software “Diffrac.Topas” (Version 5.1). The experimental conditions for all treatments, as well as the respective abbreviations, are summarized in Table 2.

Table 2: X-Ray diffraction experimental conditions.

Experiment	Abbreviation	2 Theta range	Step Size	Time per Step
Randomly oriented powder	R.O.P	From 2° to 75°	0.02	3
R. O. P. (Replicas)	R.O.P	From 2° to 75°	0.02	2
Air Dried (oriented slides)	O.S.	From 1° to 45°	0.02	2
Ethylene glycol solvated O.S.	EGOS	From 1° to 45°	0.02	2
Na- Saturation O.S.	Na-OS	From 1° to 45°	0.02	2
K Saturated+ EG O.S.	K+EG-OS	From 1° to 45°	0.02	2
Organophilic clay oriented slide	O.C	From 1° to 45°	0.02	2

2.5 Mineral quantitative analysis

Whole-rock and <1 μ m size fraction chemical compositions were assessed by X-Ray fluorescence analysis (XRF) using a Bruker’s S8 Tiger WDXRF spectrometer (Bruker Corporation, Billerica, MA, USA). Loss on ignition (LOI) was estimated for all samples and aleatory duplicates according to the following steps:

- I. Porcelain crucibles were weighed after drying in an oven at 110°C.
- II. Each crucible was labeled and filled with a powder either of whole rock or <1 μ m particle size, dried for at least 3 hrs. at 105°C and weighed. Then the dry weight of the samples was recorded.
- III. Subsequently the powders were fired for 2 hrs. at 1020°C. Finally, from the difference of the weight after drying and after firing, the LOI was estimated.

Fired powders after determination of LOI were mixed with lithium tetraborate (B₄Li₂O₇) flux.

2.6 Adsorption Experiments

All solutions were prepared using analytical grade chemicals and ultrapure water (Milli-Q Gradient System > 18 M Ω .cm). The cesium solution was prepared in an initial concentration of 1 \times 10⁻⁵ mol L⁻¹ at pH 8. A dosage of 2.5 \times 10³ mg L⁻¹ of each clay was added in centrifuge

tubes with 100 mL aliquots of the Cs solution. The tubes were then placed on an orbital shaker at a 60 rpm at room temperature. The samples were shaken continuously for a contact time of 4 days to allow sufficient time for Cs sorption onto the mineral. Mineral blanks were also tested to rule out any sorption onto container walls. After that, each tube was centrifuged for 30 minutes at 3,600 rpm in order to obtain a < 50 nm particle size cut off in the supernatant. An aliquot of the supernatant was taken from each sample and the ^{133}Cs was measured by TQ ICP-MS (Thermo Fisher ScientificTM, Bremen, Germany).

The distribution coefficient, K_d (L mg^{-1}), for each sample was calculated according to Eq. (1).

$$K_d = \frac{[\text{Cs}]_i - [\text{Cs}]_{eq}}{[\text{Cs}]_{eq}} \times \frac{1}{[\text{mineral}]} \quad (1)$$

where $[\text{Cs}]_i$ is the initial Cs concentration, $[\text{Cs}]_{eq}$ is the equilibrium Cs concentration in the aqueous phase, and $[\text{mineral}]$ is the solid-solution ratio in mg L^{-1} .

3. RESULTS AND DISCUSSION

3.1 Size distribution analysis

Size distribution analysis for all bulk samples as presented (Figure 1), yielded mean size values ranging 75 μm to 10 μm , high agglomeration and sensibility for ultrasonic treatment was observed, along with a tendency for higher size values in association to higher quartz content and lower size particle mean value in correlation to may minerals overall content.

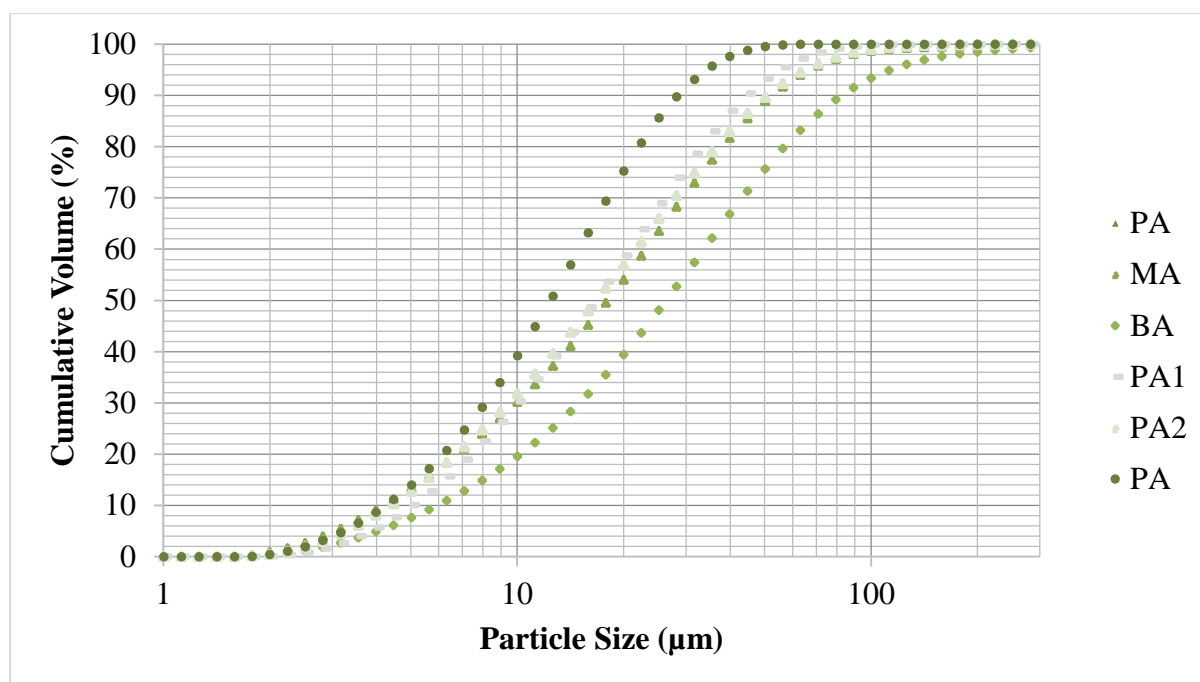


Figure 1: Size distribution analysis of all samples.

The graph above shows that the PA samples are composed in higher proportions (60 %) of particles of approximately 25 μm , whereas 50 % of the BA studied sample has around 50 μm .

3.2 Geochemical information

Results from XRF chemical analysis on the whole-rock samples are presented in table 4, and they offer a chemical composition in agreement with what can be expected from parent rock and genesis mode. Moreover, Fe_2O_3 and SiO_2 contents from bulk chemistry shown in Table 4, 3, allowing deductions on the geochemical affinity with respect to the parent rock. Smectites derived from basic rocks may have three times the Iron content forming than those of intermediate to basic volcanic source, and they tend to alter into Fe-Montmorillonites and Fe-beidellites, as it is the case for samples coming from Paraiba and particularly Maranhão.

Silica levels in a lesser extent may also indicate the acid to basic parent rock, tending towards intermediate to acidic in higher SiO_2 contents, and lower contents derived from basic composition extrusive rocks. Samples PA2 and MA showed higher Fe_2O_3 values and relatively lower SiO_2 , which seems to indicate that they are basaltic precursors (Table 4).

Table 3: Whole rock chemical composition from XRF fused beads 10 major elements.

sample	Wt%											$\Sigma(\text{Sum})$
	SiO ₂	Al ₂ O ₃	Fe ₂ O ₃	MnO	MgO	CaO	Na ₂ O	K ₂ O	TiO ₂	P ₂ O ₅	LOI	
PA	66,07	16,08	5,74	0,05	1,67	0,51	0,68	2,02	0,86	0,05	6,26	99,97
BA	56,69	19,72	9,21	0,11	3,47	0,38	0,08	0,04	0,40	0,05	10,20	100,35
PA2	56,37	21,16	8,09	0,01	3,70	0,13	0,08	0,04	0,39	0,01	10,10	100,08
PA2	62,82	13,94	8,20	0,03	2,53	2,51	0,61	0,22	0,75	0,04	8,16	99,81
MA	46,91	20,62	16,95	0,19	2,94	0,51	0,01	0,97	1,72	0,03	10,02	100,86

Feldspar species and Hematite appear to be the source of major concern for chemical interference with respect to the geo-barrier performance, in the sense that they offer higher solubility and via means of cation exchange with free K may induce lamellar collapse (illitization) as a function of time in an hydrothermal environment, as could be the case for samples PA & MA.

3.3 Mineral phase identification and quantification

From randomly oriented XRD traces refined under Rietveld methodology, the next chart (Table 3) summarizes the mineralogical composition for all samples.

Table 4: Quantitative mineral analysis results, after crosschecking Rietveld-Topas results against XRF-XRF molar sum.

Mineral	Sample	PA	MA	BA	PA1	PA2
<i>Montmorillonite</i>		29,4	64,5	83,0	55,0	50,0
<i>Quartz</i>		21,2		1,0	38,0	30,0
<i>Hematite</i>			6,8	1,0		
<i>Kaolinite</i>		6,9	23,3	13,0		19,0
<i>Illite</i>		19,3				
<i>Albite</i>		11,7	5,4			
<i>Cristobalite</i>						
<i>K-Felspar</i>		8,0		2,0		
<i>Anortite</i>					3,0	1,0
<i>Graphite</i>		2,5			4,0	
<i>Olivine</i>		1,1				
	SUM	100,0	100,0	100,0	100,0	100,0

3.4 Cs Adsorption

All samples were tested for in ¹³³Cs adsorption capability in aqueous media, results indicated that all adsorbents were effective in removing the target metal (Figure 2). PA1 was the most effective adsorbent with 88% of cesium removal, and shares a similar performance with PA2 from the same region, although smectite content for both of this samples is not the highest among the set, it can be expected that agglomeration presented as an smectite coating over

quartz's large particles, in a low agitation energy system may favour mesoporous interactions, PA1 is presumably enhanced for containing higher Na^+ cations in interlayer position, not containing kaolinite and possibly graphite is well known to be a sorptive media.

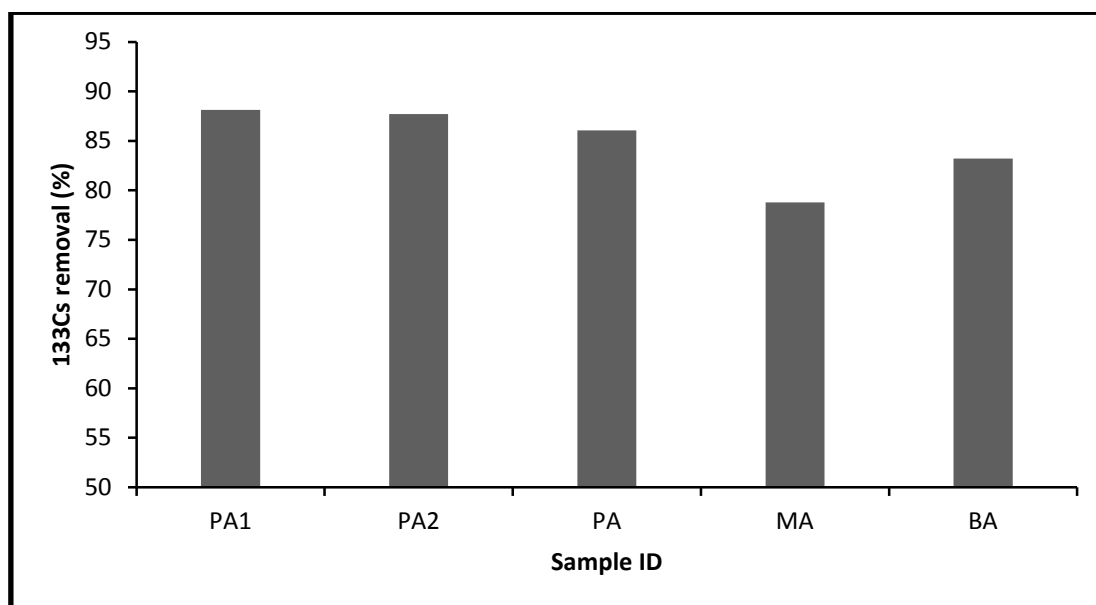


Figure 2: Adsorbents used in ^{133}Cs sorption. $[^{133}\text{Cs}]_0 = 1.02 \text{ mg L}^{-1}$

On the other hand, MA presented the lowest value, which was 79% possibly due to very high layer charge Fe^+ smectites and the presence of Iron phases mostly hematite, creating an electrostatic repulsive aqueous interaction in the experimental setup. Figure 3 presents the adsorption data in terms of the logarithm of the distribution coefficient ($\ln(K_d)$) versus the logarithm of the equilibrium aqueous Cs concentration ($\ln[^{133}\text{Cs}_{eq}]$).

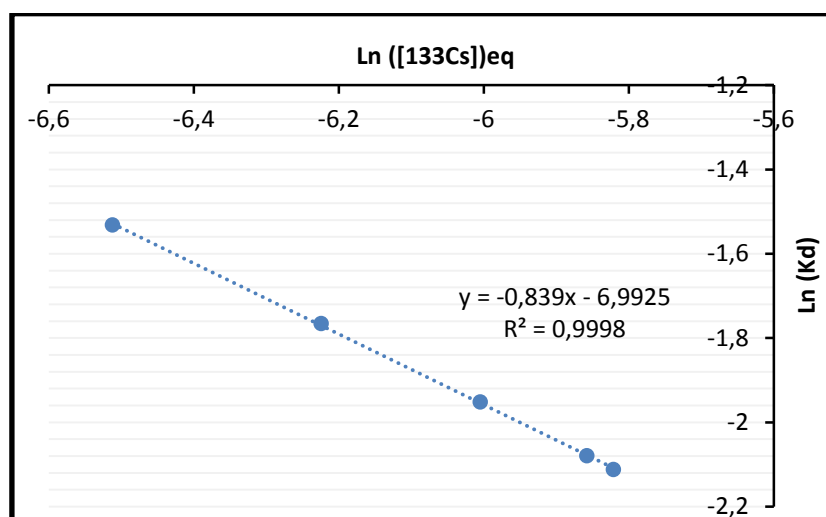


Figure 3: Relationship between K_d and $^{133}\text{Cs}_{eq}$

The relation between cesium concentration at equilibrium and the distribution coefficient was linear (inversely proportional), as indicated by Figure 3, with a correlation coefficient (R^2) of 0.9998. The highest k_d value was obtained for PA1, with $2.96 \times 10^{-3} \text{ L mg}^{-1}$. This value is

two-fold higher than that obtained by MA. These preliminary results indicate PA1 as the best option regarding cesium adsorption.

4. CONCLUSIONS

This may be a first step aiming to fully develop a comparative perspective of local prospects for clay buffer, applied for radioactive waste management; fundamental parameters are yet to be studied such as diffusion, geotechnical properties and compatibility, regularity of the mineral reserves, state priorities and regulatory aspects concerning international nuclear energy establishments. Nevertheless, results thus far indicate that moderate grade bentonites could be a suitable material for barrier in a LILW design, natural bentonite and sand mix could in certain type of constructive approaches constitute the most compressible materials and offering the possibility of controlled self-locking/sealing engineered barrier after in situ hydraulic swelling. The crystal chemistry of smectite species showed to be a sensible parameter with respect to isomorphic substitutions, particularity in the case of Fe^{2/3} commonly located in octahedral positions regardless of oxidation state.

ACKNOWLEDGMENTS

We the authors would like to express our gratitude to the *Coordenação de Aperfeiçoamento de Pessoal de Nível Superior* (CAPES) for providing financial support to this research project, the university of Sao Paulo and specially the research units: Larex, *laboratorio de caracterizcao tecnologica* (LCT) and the *Instituto de Pesquisas Energéticas e Nucleares* (IPEN / CNEN - SP).

REFERENCES

1. Nuclear Fuel Cycle Royal Commission. "Management, Storage and Disposal of Nuclear and Radioactive Waste," <http://nuclearrc.sa.gov.au/app/uploads/2015/04/Issues-Paper-Management-Storage-and-Disposal-of-Waste1.pdf> (2015).
2. R. Pusch. "Clays and Nuclear Waste Management," Chapter 11.4. In: F. Bergaya, B. K. G. Theng and G. Lagaly. "Handbook of Clay Science", Elsevier (2006).
3. International Atomic Energy Agency. "Low and Intermediate Level Waste Repositories: Socioeconomic and Public Involvement," IAEA-TECDOC-1553. *Proceedings of a workshop held in Vienna*, November 9-11 (2005).
4. Comissão Nacional de Energia Nuclear. "Programa Política Nuclear: PPA 2016-2019 e LOA 2016," <http://www.cnen.gov.br/images/cnen/documentos/planejamento/ProgramaPoliticaNuclear-PPA-2016-2019.pdf> (2016).
5. Ministério da Ciência, Tecnologia, Inovação e Comunicações. "Relatório de Gestão do Exercício de 2016 - TCU, Brasília, DF," <https://www.mctic.gov.br/mctic/export/sites/institucional/transparencia/arquivos/Relatorio-de-Gestao-2016.pdf> (2017).

6. M. Chino, H. Nakayama, H. Nagai, H. Terada, G. Katata, and H. Yamazawa. "Preliminary estimation of release amounts of ¹³¹I and ¹³⁷Cs accidentally discharged from the Fukushima Daiichi nuclear power plant into the atmosphere," *Journal of Nuclear Science and Technology*, **v. 48**, pp. 1129–1134 (2011).
7. R. C. Hoetzlein. "Visual communication in times of crisis: The Fukushima nuclear accident," *Leonardo*, **v. 45**, pp. 113–118 (2012).
8. T. J. Yasunari, A. Stohl, R. S. Hayano, J. F. Burkhart, S. Eckhardt, and T. Yasunari. "Cesium-137 deposition and contamination of Japanese soils due to the Fukushima nuclear accident," *Proceedings of the National Academy of Sciences of the USA*, **v. 108**, pp. 19530–19534 (2011).
9. K. Buesseler, M. Aoyama, and M. Fukasawa. "Impacts of the Fukushima Nuclear Power Plants on Marine Radioactivity," *Environ. Sci. Technol.*, **v. 45**, n. 23, pp. 9931-9935 (2011).
10. G. Marović, T. Bituh, Z. Franić, I. Gospodarić, J. Kovać, N. Lokobauer, M. Maracić, B. Petrinc and J. Senćar. "Results of environmental radioactivity measurements in the Republic of Croatia, annual reports 1998–2009," *Institute for Medical Research and Occupational Health* (2010).
11. Z. Franic and B. Petrinc. "Marine radioecology and waste management in the Adriatic," *Archives of Industrial Hygiene and Toxicology*, **v. 57**, pp. 347–352. (2006).
12. T. Y. Tang, J. H. Tai, and Y. J. Yang. "The flow pattern north of Taiwan and the migration of the Kuroshio," *Continental Shelf Research*, **v. 20**, pp. 349–371 (2000).
13. D. Dermatas, M. Chrysochoou, S. Pardali, D. G. Grubb. "Influence of X-Ray Diffraction Sample Preparation on Quantitative Mineralogy," *J. Environ. Qual.*, **v. 36**, n. 487 (2007).
14. B. H. O'Connor, W. -J. Chang. "The amorphous character and particle size distributions of powders produced with the Micronizing Mill for quantitative x-ray powder diffractometry," *X-Ray Spectrom*, **v. 15**, pp. 267–270 (1986).
15. R. Kleeberg, T. Monecke, S. Hillier. "Preferred orientation of mineral grains in sample mounts for quantitative XRD measurements: How random are powder samples?," *Clays Clay Miner.*, **v. 56**, pp. 404–415 (2008).
16. D. M. Moore, R. C. J. Reynolds, *X-Ray Diffraction and the Identification and Analysis of Clay Minerals*, Oxford University Press, New York, USA (1997).
17. S. J. Chipera, D. L. Bish. "Baseline studies of the clay minerals society source clays: Powder X-ray diffraction analyses," *Clays Clay Miner.*, **v. 49**, pp. 398–409 (2001).